Laboratori Nazionali di Frascati

LNF-69/55

G. Gialanella, A. Piazza, G. Susinno, L. Fiore and G. C. Mantovani :
ANALYSIS OFT HE REACTION $\gamma+p \rightarrow p+\pi^{+}+\pi^{-}$ AT ENERGIES UP TO 1 GeV IN A HYDROGEN BUBBLE CHAMBER.

Estrattp da : Nuovo Cimento 63a, 892 (1969)

G. GIALANELLA, *et al.*
1° Ottobre 1969
Il Nuovo Cimento
Serie X, Vol. 63 A, pag. 892-914

Analysis of the Reaction $\gamma+p \to p+\pi^+ +\pi^-$ at Energies up to 1 GeV in a Hydrogen Bubble Chamber.

G. GIALANELLA

Istituto di Fisica dell'Università - Roma
Istituto Nazionale di Fisica Nucleare - Sezione di Roma

A. PIAZZA and G. SUSINNO

Laboratori Nazionali del CNEN - Frascati

L. FIORE

Istituto di Fisica dell'Università - Roma

G. C. MANTOVANI

Istituto di Fisica dell'Università - Pavia
Istituto Nazionale di Fisica Nucleare - Gruppo di Pavia

(ricevuto il 21 Maggio 1969)

Summary. — The final result of an experiment of double charged-pion photoproduction on proton up to 1 GeV are reported. The most striking feature is the very abundant production of the Δ-isobar in the $\Delta^{++}(\pi^+p)$ charge state and the very low production percentage of its neutral charge state (π^-p). This fact, together with the evident peak of the total cross-section at $E_\gamma = 650$ MeV, suggests trying to fit the data with an isobar excitation model, the intermediate state having $T = \frac{1}{2}$. However, definite conclusions on the formation of the P_{11} resonance cannot be drawn. A good fit of the angular distributions of the Δ^{++} production is obtained with second-order polynomials in cos θ. The mass distribution of the $(\pi^+\pi^-)$ system does not show any enhancement, which may be attributed to a $(\pi^+\pi^-)$ resonance with mass below 600 MeV/c^2.

1. – Introduction.

The present analysis of the reaction

(1) $$\gamma+p \to p+\pi^+ +\pi^-$$

is a part of a systematic investigation of photoproduction reactions on proton and neutron with more than two bodies in the final state, undertaken at Frascati using the bubble chamber technique. The purpose is to get further information about the photoproduction mechanism below 1 GeV.

In the past the reaction (1) was analysed mainly with counter techniques. Only recently a collection of data with considerable statistics was obtained in bubble chamber experiments at the CEA and DESY laboratories [1,2]. Some preliminary results of our experiment have been reported in ref. [3].

The present status of the phenomenological analysis of the data concerning the reaction (1) can be summarized as follows.

Because of the very abundant production of Δ-isobar ($\mathcal{N}_{33}(1238)$), at least below 1.1 GeV, the CEA group tried to interpret the data in terms of an isobar excitation mechanism, assuming that reaction (1) goes according to the scheme

$$\gamma+p\to\mathcal{N}^*_{\frac{1}{2}}\to\Delta+\pi\,, \tag{2}$$

where $\mathcal{N}^*_{\frac{1}{2}}$ is a mixture of the known $T=\frac{1}{2}$ resonances P_{11}, D_{13}, F_{15}.

A best fit of the total production cross-section gave the relative strengths of the three isobars which can be involved in reaction (2). Such a fit, however, is not very sensitive to the eventual presence of nonresonant contributions, which could appreciably modify the angular distributions. On the other hand, the experimental angular distributions are not very sensitive to the relative strength of the various isobars. Furthermore, it seems unreasonable to neglect any contribution of the OPE model, although the peripheral mechanism alone cannot account for experimental data at low energies.

According to the above considerations, the DESY group tried to interpret the data with an improved model [4], which included a small admixture of isobaric contribution in the gauge invariant extended OPE model [5].

Now, while the predictions of both models agree satisfactorily on the main

---

(1) CAMBRIDGE BUBBLE CHAMBER GROUP. *Phys. Rev. Lett.*, 13, 636, 640 (1964); *Proc. Intern. Symp. on Electron and Photon Interactions at High Energies*, vol. 2 (Hamburg, 1965), p. 21; *Phys. Rev.*, **146**, 994 (1966); **155**, 1468, 1477 (1967); 156, 1426 (1967); **163**, 1510 (1967).

(2) AACHEN, BERLIN, BONN, HAMBURG, HEIDELBERG, MÜNCHEN COLLABORATION *Proc. Intern. Symp. on Electron and Photon Interactions at High Energies*, vol. 2 (Hamburg, 1965), p. 36; *Nuovo Cimento*, **41** A, 270 (1966); **48** A, 262 (1967); **49** A, 504 (1967); *Phys. Lett.*, 83, 707 (1966); *Nucl. Phys.*, **1** B, 668 (1967); *Phys. Rev.*, **175**, 1669 (1968).

(3) S. DE SCHRYVER, L. FIORE, S. FOCARDI, G. GIALANELLA, V. ROSSI, B. STELLA and G. SUSINNO: Frascati Report LNF-68/21 (1968); L. FIORE, G. GIALANELLA, V. ROSSI, S. DE SCHRYVER, A. PIAZZA, B. STELLA, G. SUSINNO, S. FOCARDI and G. C. MANTOVANI: *Nuovo Cimento*, **56** A, 1099 (1968).

(4) D. LÜKE, M. SCHEUNERT and P. STICHEL: *Nuovo Cimento*, **58** A, 234 (1968).

(5) P. STICHEL and M. SCHOLZ: *Nuovo Cimento*, **34**, 1388 (1964).

features of doubly charged photoproduction, there are still some discrepancies in the quantitative predictions. For this reason and because all model assumptions were done essentially to explain the data of reaction (1), it seems important to analyse processes of double photoproduction with different final states.

The present paper consists of six parts. In Sect. **2** we describe the experimental apparatus and the exposing procedure; in Sect. **3** we report the cross-sections and the kinematical distributions. The production of Δ-isobar and the two-pion system are analysed in Sect. **4** and **5** respectively. Our conclusions are reported in Sect. **6**.

2. – Experimental apparatus and exposing procedure.

2·1. *The bubble chamber.* – The hydrogen bubble chamber used was constructed at the CERN laboratories and operated there until 1962. In 1965 it was carried to the Laboratori Nazionali di Frascati.

The chamber has a cylindrical body with a 32 cm diameter, a 15 cm depth and is placed in a 17 kG magnetic field. The main modification introduced for this experiment is the beam entrance window. It consists of a 0.25 mm thick mylar sheet ((6×1) cm^2), in order to minimize the electromagnetic background. In this way the beam, before entering the chamber, passes through about 10^{-3} radiation lengths, which corresponds to $\frac{1}{30}$ of the hydrogen thickness in the chamber.

For safety reasons the window is enclosed in a 3.5 m long stainless steel tube, which, in the case of breaking of the mylar window, prevents the hydrogen from escaping. The electromagnetic background produced in the 0.5 mm thick plug of the tube is removed by a clearing magnetic field and by a collimator placed in the tube itself.

The 17 kG analysing magnet was powered by a Graetz bridge rectifier using silicon diodes. To overcome the lack of current stabilization, a Hall field meter was introduced in the magnet and its output, in digital form, was photographed on every picture.

2·2. *Beam set-up.* – In Fig. 1 the experimental lay-out is shown. The bremsstrahlung beam was produced by spilling the circulating electrons in the synchrotron onto a 0.1 radiation length tantalium target. Compatibility with simultaneous beam users was achieved by setting up the target every time with a suitable current pulse synchronized with the bubble chamber expansion.

The photon beam was hardened by means of 4 radiation lengths of LiH, which also reduced its intensity to more suitable values, while maintaining the maximum circulating beam current in the synchrotron. The beam size at the chamber entrance was (3.0×0.4) cm^2.

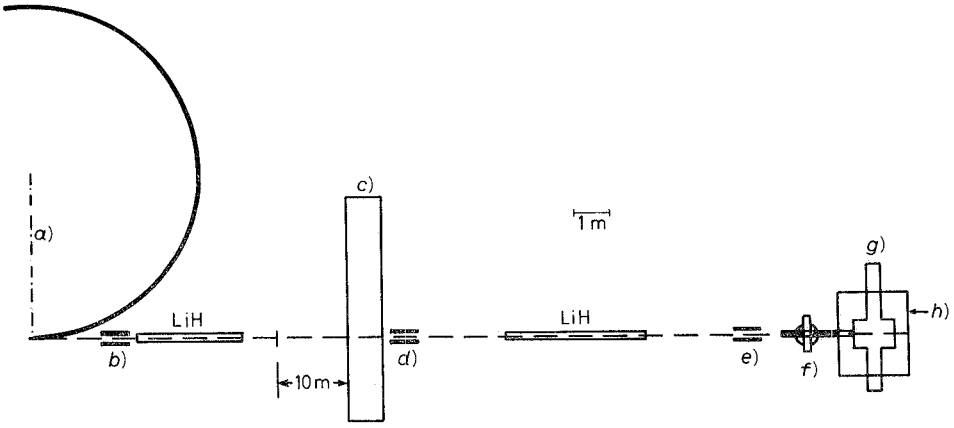

Fig. 1. – Experimental lay-out. *a*) Synchrotron; *b*), *d*), *e*) collimator; *c*) shielding; *f*) sweep magnet; *g*) bubble chamber; *h*) magnet.

The γ-ray spectrum, obtained by measuring the momenta and angles of the e^+e^- pairs produced in the chamber, is shown in Fig. 2. As one can see, the hardener thickness, chosen in order to obtain the best photon-beam intensity,

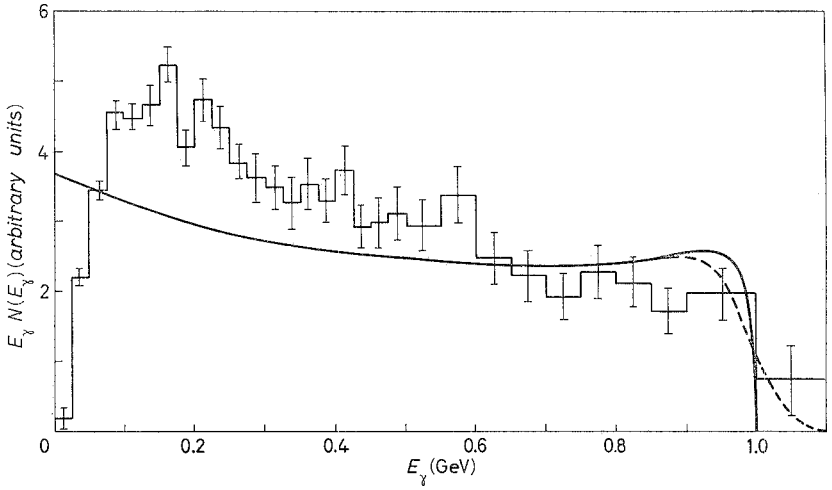

Fig. 2. – Photon spectrum. The continuous curve represents the calculated bremsstrahlung spectrum and is normalized to the experimental spectrum above 500 MeV. The errors shown are statistical.

was probably too high; in fact, a regeneration of photons with intermediate energies, due to the secondary bremsstrahlung process taking place in the adsorber itself, is evident. The continuous line represents the theoretical bremsstrahlung spectrum normalized to the measured values above 500 MeV. The maximum photon energy was 1 GeV.

The photon flux was adjusted to about 300 equivalent quanta per pulse, corresponding to about 10 e^+e^- pairs per picture. The total number of incident γ-rays was obtained in a part of the film by counting the e^+e^- pairs in a sample of pictures and on the other part by means of an external monitoring systems.

2·3. *Scanning and measuring procedure.* – About 400 000 pictures were taken with the previously described photon beam. All the film was scanned twice giving an overall efficiency of about 99% (90% for each scanning). The searched events were easily distinguishable from the electromagnetic background, because of the presence of three prongs, one of which, the proton, was almost always very ionizing.

The measurements were carried out with conventional digitized apparatus yielding a standard deviation on the point measurements of 0.1 mm in the real space. The geometrical reconstruction of the events and the kinematical calculations were accomplished with the standard THRESH and GRIND programs.

The events were accepted in a fiducial volume having the same section of the photon beam and extending 20 cm along its direction. This ensures that all tracks had sufficient length to permit a good measurement.

2·4. *Analysis of the events.* – Since in the 3-prong events under study the angles and momenta of the three charged particles, as well as the direction of the incoming photon and all the masses, were known, the kinematics of the investigated reaction was over-determined and a $3C$-fit was possible.

The events were accepted only after controlling the bubble density on the film. In Fig. 3 the experimental distribution of the χ^2 resulting from the $3C$-fit is shown. The events were accepted only if $\chi^2 \leqslant 12$.

The total number of selected events of reaction (1) was 2864. These events have been divided in 10 intervals of incident γ-ray energy. Table I shows the number of the events found in each energy interval.

TABLE I.

Interval	E_γ (MeV)	No. of events
I	350 ÷ 500	189
II	500 ÷ 550	288
III	550 ÷ 600	397
IV	600 ÷ 650	375
V	650 ÷ 700	355
VI	700 ÷ 750	290
VII	750 ÷ 800	245
VIII	800 ÷ 850	241
IX	850 ÷ 900	203
X	900 ÷ 1000	275

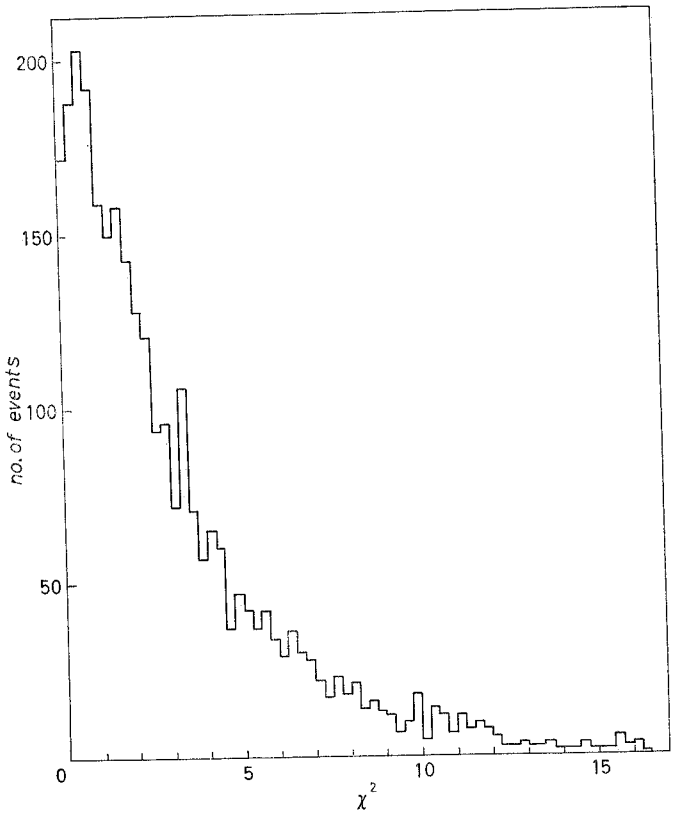

Fig. 3. χ-square experimental distribution for all 3-C events.

3. – Cross-sections and kinematical distributions.

The total cross-section, reported in Fig. 4, increases rapidly with energy up to 650 MeV and then remains almost constant, in agreement with the previous bubble chamber results ([1,2]). The quoted errors include the statistical error of the sample of events and the statistical error of the sample of pairs from which the photon spectrum was derived.

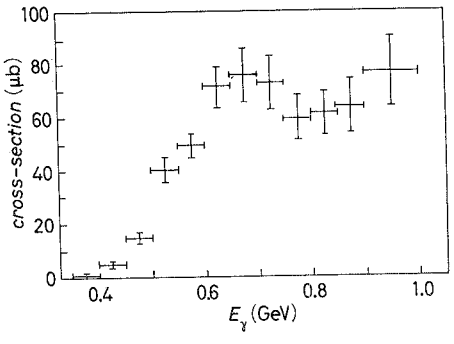

Fig. 4. – Total cross-section for the reaction $\gamma+p\to p+\pi^+ +\pi^-$. The errors quoted include the statistical error of the sample of events and the statistical error of the sample of pairs, used to determine the photon spectrum.

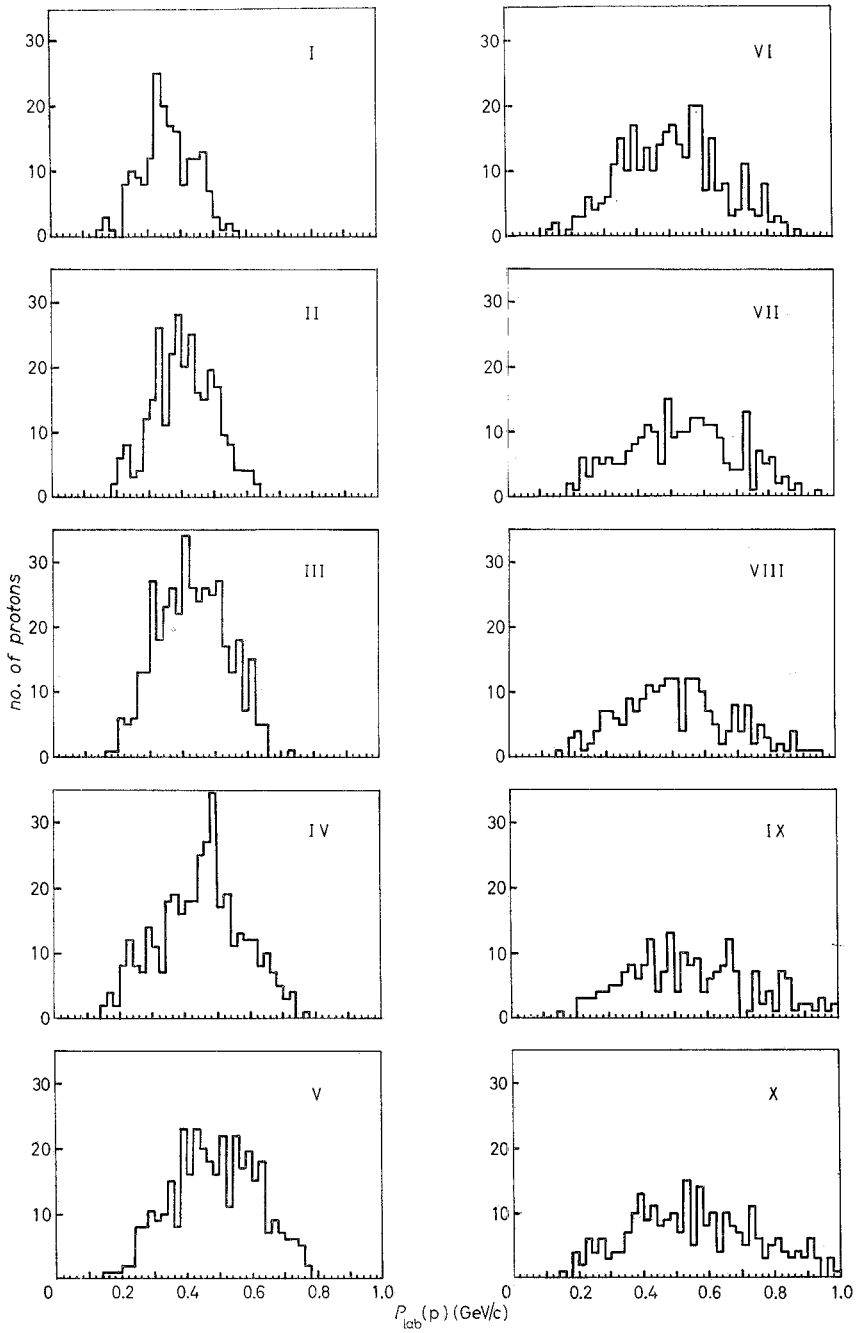

Fig. 5. – Distribution of the proton momentum for the various photon energy intervals of Table I.

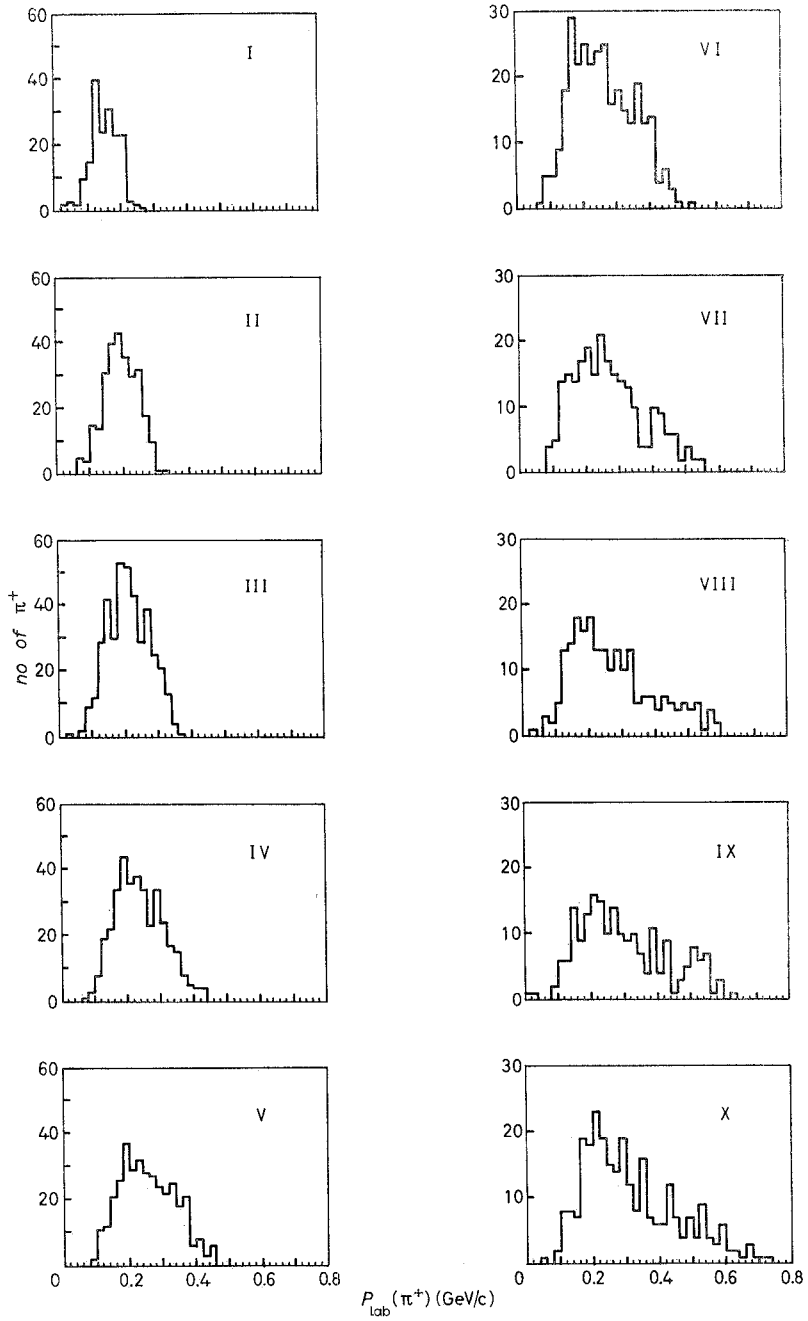

Fig. 6. – Distribution of the π^+ momentum for the various photon energy intervals of Table I.

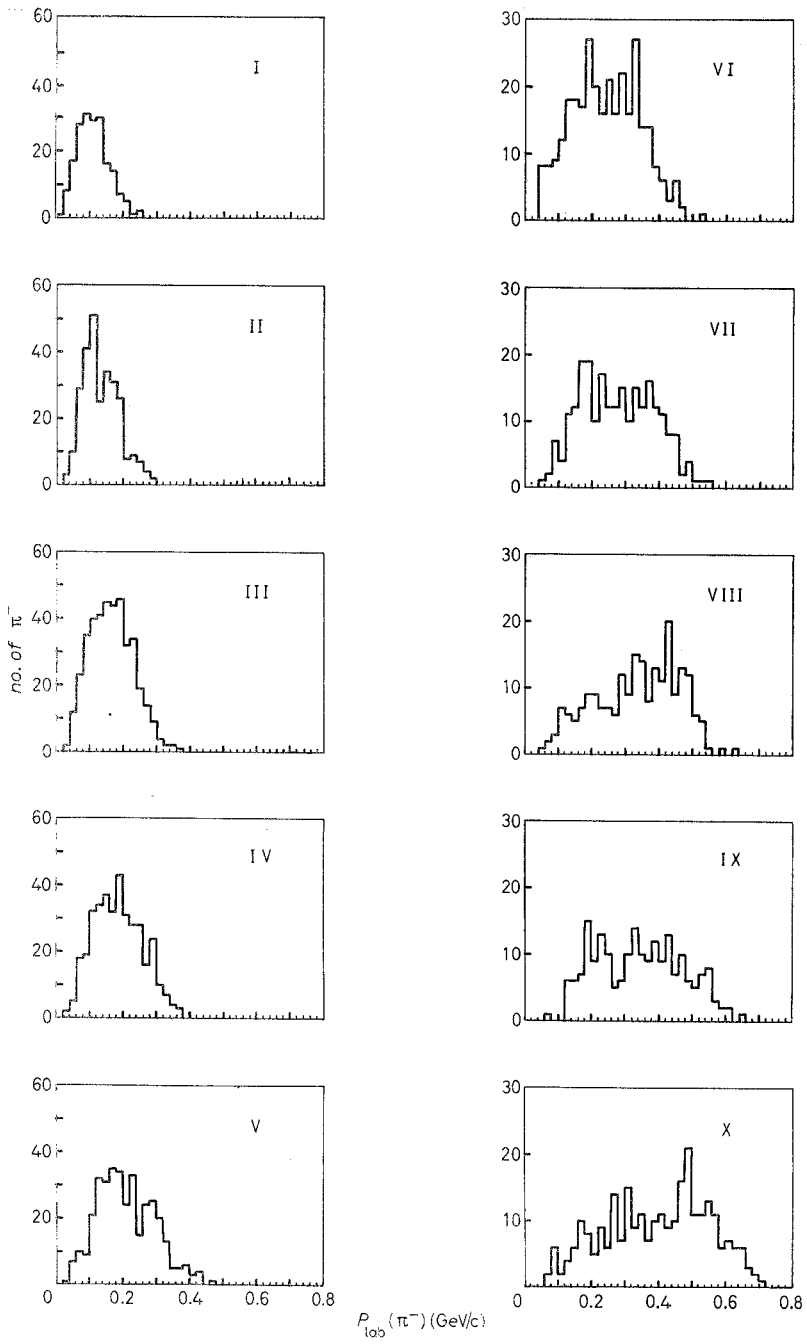

Fig. 7. – Distribution of the π^- momentum for the various photon energy intervals of Table I.

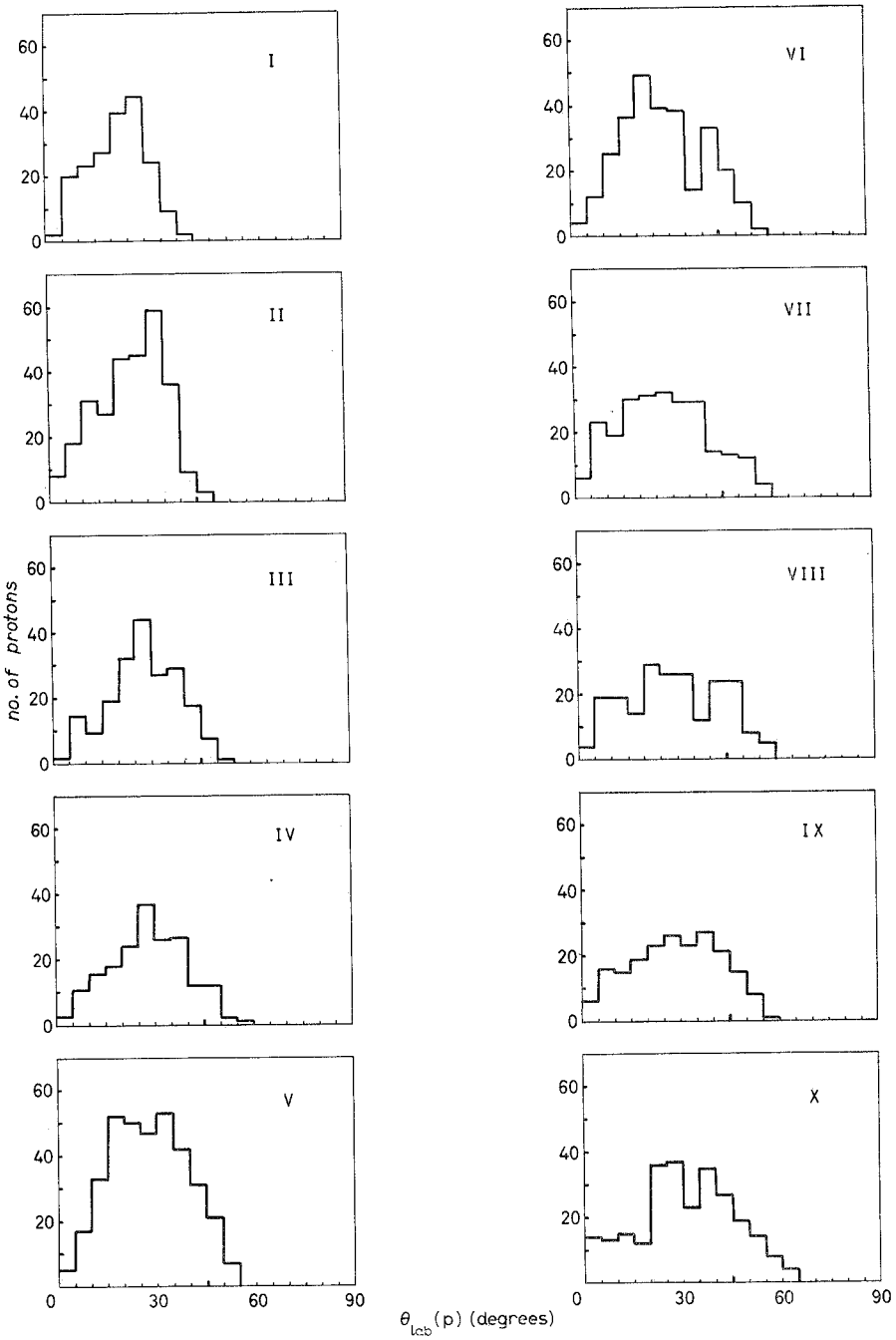

Fig. 8. – Distribution of the angle θ_p between the proton and photon directions in the laboratory system for the various photon energy intervals of Table I.

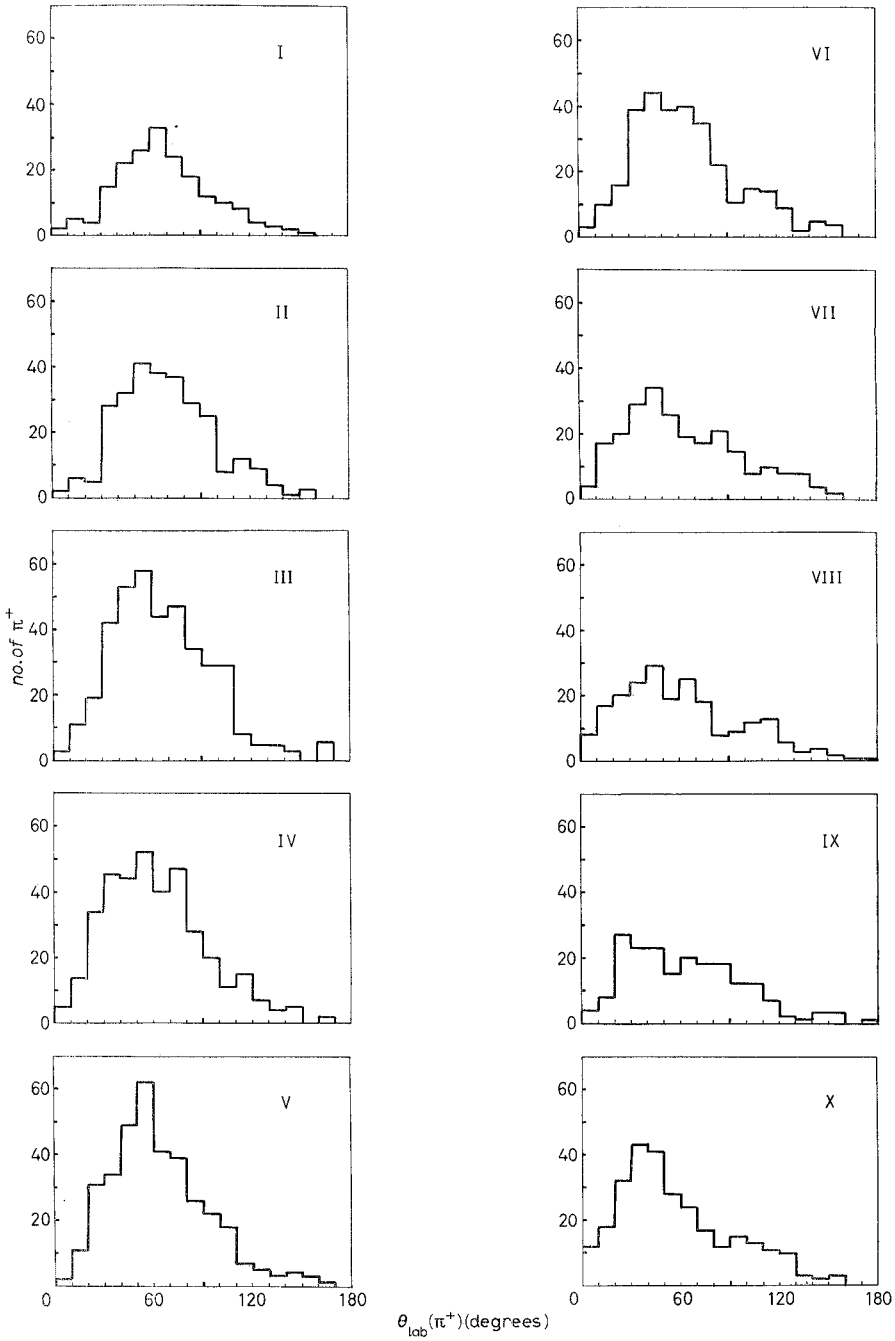

Fig. 9. – Distribution of the angle θ_{π^+} between the π^+ and photon directions in the laboratory system for the various photon energy intervals of Table I.

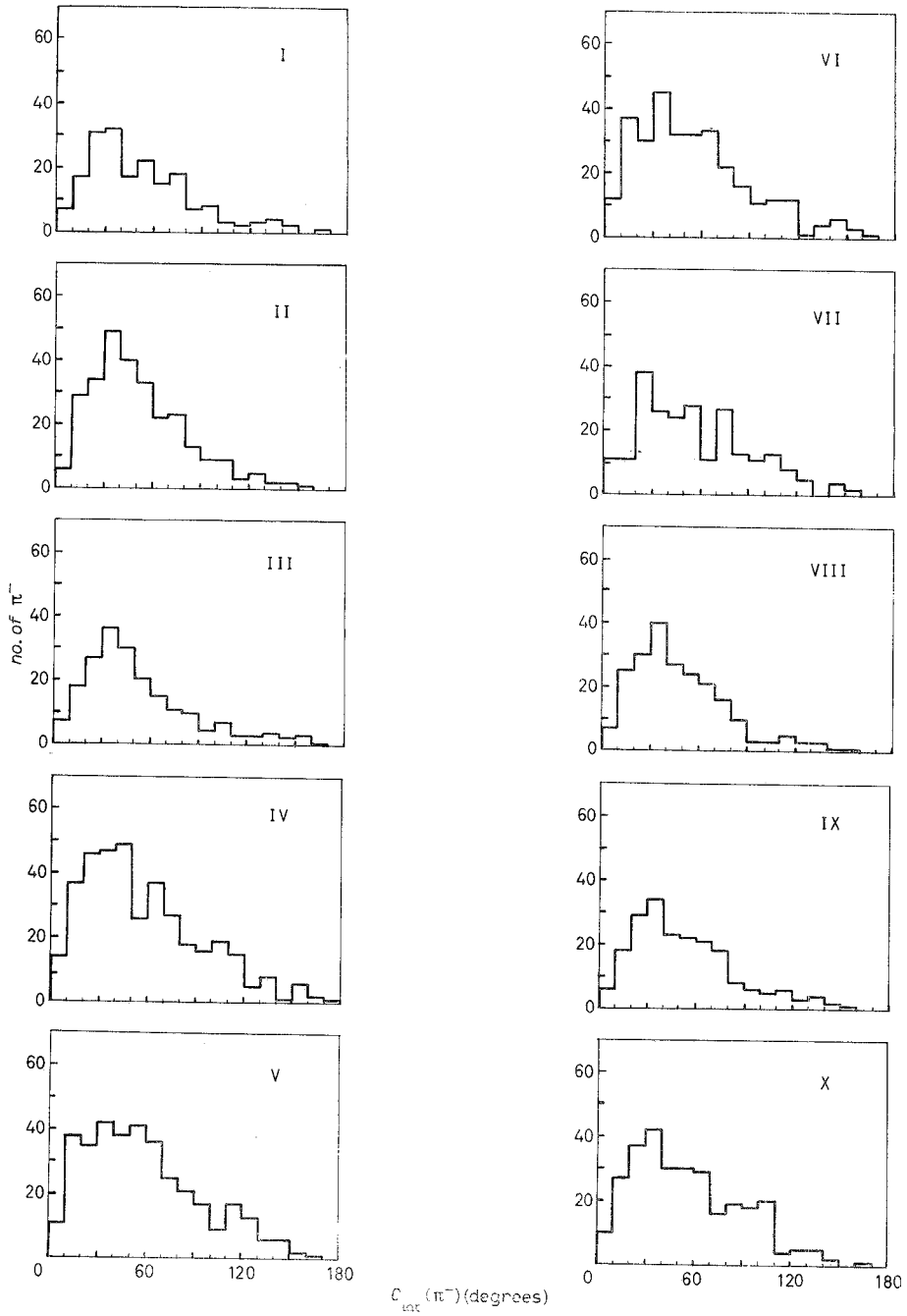

Fig. 10. – Distribution of the angle θ_{π^-} between the π^- and photon directions in the laboratory system for the various photon energy intervals of Table I.

In Fig. 5, 6 and 7 the laboratory momentum distribution of the three charged particles in each photon energy interval are reported, while Fig. 8, 9 and 10 show the corresponding angular distributions. These distributions represent the actual behaviour of the kinematics of the reaction (1), taking into account the dynamics of the reaction and all final-state interactions.

4. – The $\Delta(1236)$-isobar production.

4·1. *Equivalent mass distributions and production total cross-section.* – The main characteristic of reaction (1) is the very abundant production of the $\Delta^{++}(1236)$-

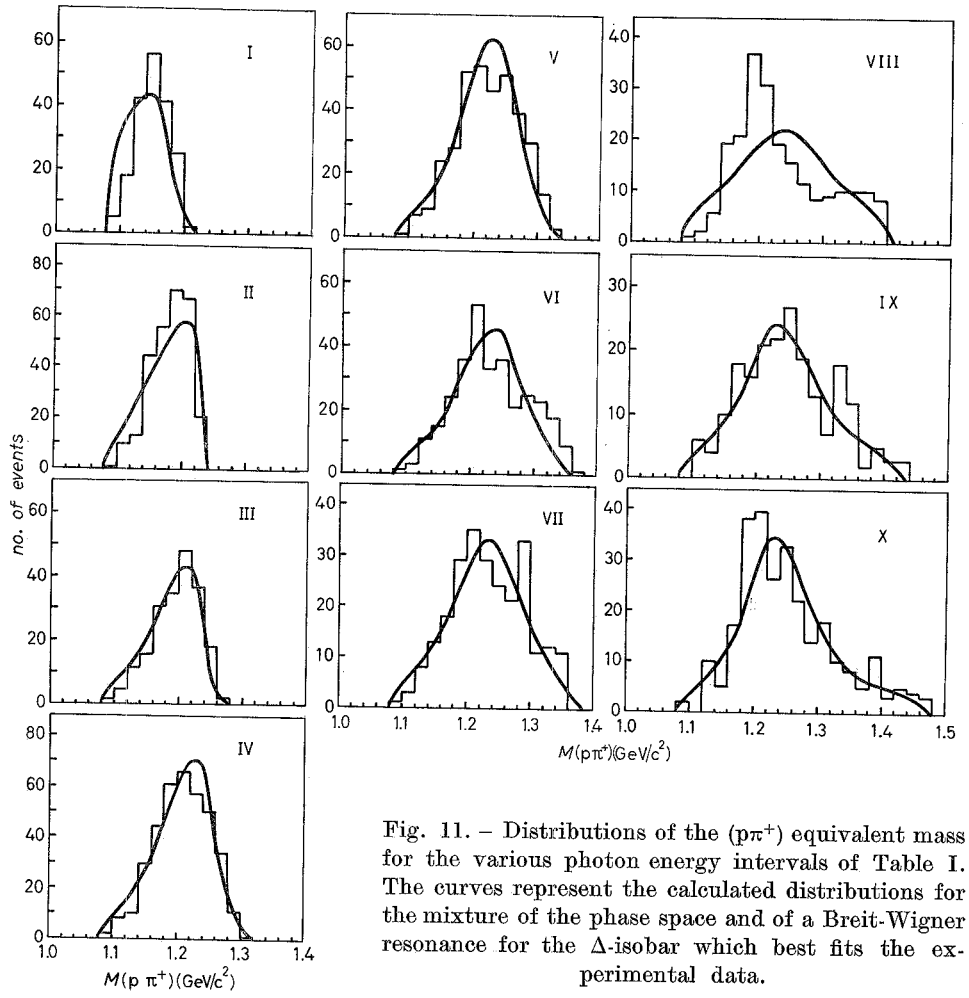

Fig. 11. – Distributions of the $(p\pi^+)$ equivalent mass for the various photon energy intervals of Table I. The curves represent the calculated distributions for the mixture of the phase space and of a Breit-Wigner resonance for the Δ-isobar which best fits the experimental data.

isobar. In Fig. 11, the mass distributions of the $(p\pi^+)$ system, in the different energy intervals, are shown. We tried to fit these distributions by superimposing a Breit-Wigner for the isobar to the phase-space distribution. This procedure implies the assumption that there is no contribution from the $\Delta^0(p\pi^-)$ production. This assumption, indeed, is supported by the good fit of the $(p\pi^-)$ mass distribution, obtained by taking into account the only Δ^{++} reflection added to the phase-space distribution. No attempt was made to introduce in the fit a possible interference between the two charge states of the Δ-isobar. The results of the fit are summarized in Fig. 12. The production percentage of the Δ^{++} is 100% up to $E_\gamma = 650$ MeV and then decreases to about 75%. Between 800 and 850 MeV the obtained value is much lower than reasonably expected. This anomalous value is related to the displacement of the Δ peak in the mass distribution, whose origin we are unable to explain. Indeed, we want to stress out that in this energy interval (about 800 MeV) there seems to be some strange effect in our experimental data.

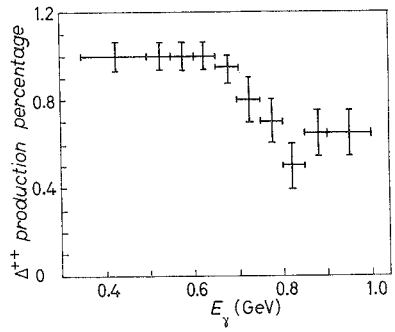

Fig. 12. – Δ^{++}-isobar production percentages *vs.* E_γ as resulting from the best fit of the (π^+p) and (π^-p) mass distribution.

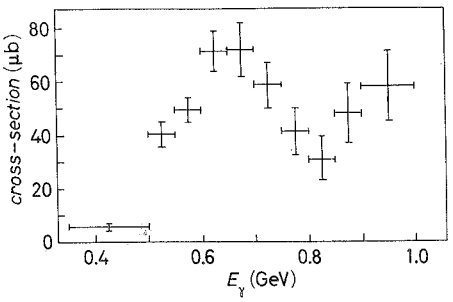

Fig. 13. – Total cross-section for the reaction $\gamma+p\to\Delta^{++}+\pi^-$.

The total Δ^{++}-isobar production cross-section is shown in Fig. 13. The mass distribution for the $(p\pi^-)$ system was calculated by superimposing the Δ^{++} reflection to the phase-space distribution. The calculated and experimental distributions are shown in Fig. 14.

4·2. *Production angular distributions.* – Since the main characteristic of reaction (1) consists in going essentially through the reaction (2), the production angular distribution can give information on the angular momenta of the waves involved in the process. In Fig. 15 the differential cross-sections for the various photon energy intervals are given. The plotted events are those for which $1.15\ \text{GeV}/c^2 \leqslant M(p\pi^+) \leqslant 1.30\ \text{GeV}/c^2$.

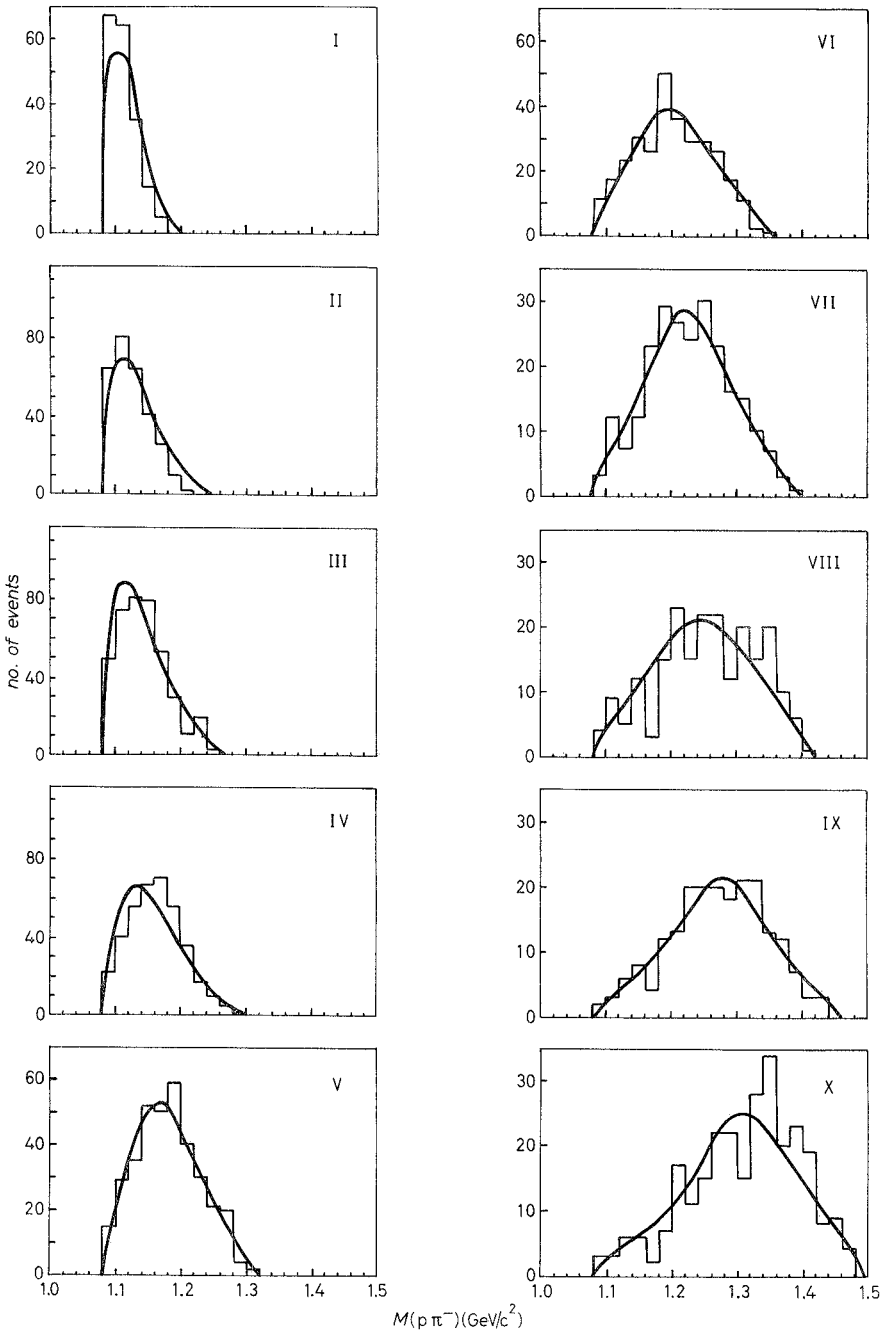

Fig. 14. – Distributions of the ($p\pi^-$) equivalent mass for the various photon energy intervals of Table I. The curves represent the calculated distributions, taking into account the reflection of the Δ^{++}-isobar.

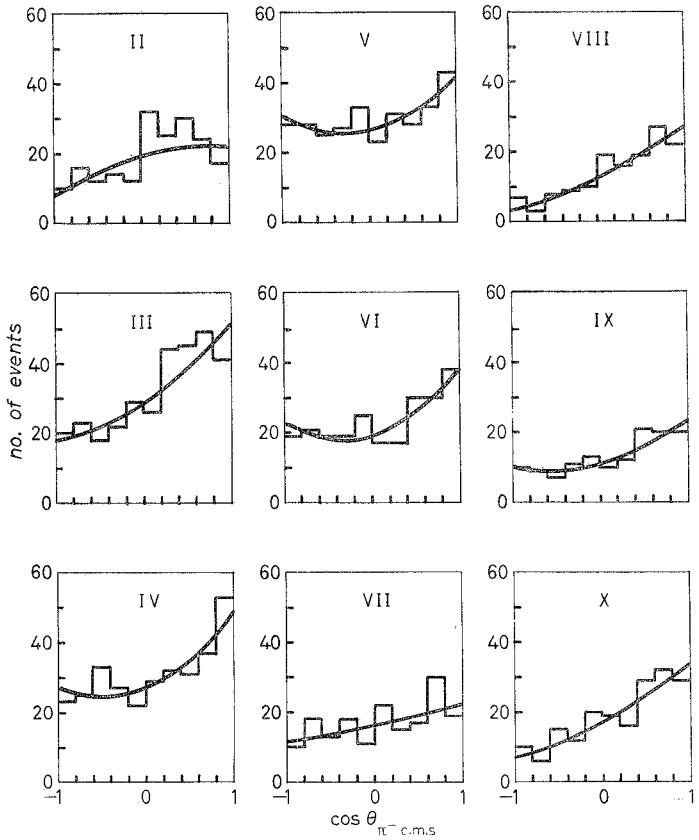

Fig. 15. – Angular distribution of the π^- in the reaction $\gamma+p\to\Delta^{++}+\pi^-$ for the various photon energy intervals of Table I. θ_{π^-} is the angle, in the c.m.s., between the incoming photon and the outgoing π^-. The curves represent the result of the polynomial fit.

Good fits were obtained with second-order polynomials of the type

$$\sigma(\theta) = A_0 + A_1\cos\theta + A_2\cos^2\theta \tag{3}$$

in all the energy intervals (θ being the angle in the c.m.s. between the incoming photon and the outgoing π^-).

A fit with higher-order polynomials was also tried to take into account the

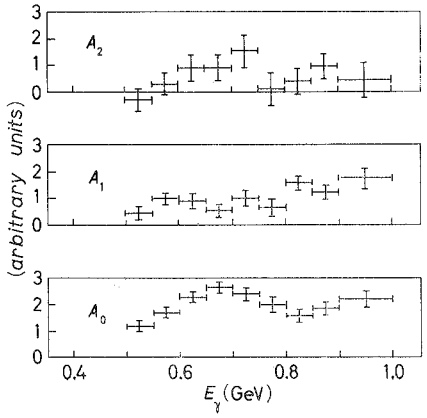

Fig. 16. – Behaviour of the coefficients of the expansion in $\cos\theta$ polynomials of the c.m. angular distribution for the reaction $\gamma+p\to\Delta^{++}+\pi^-$.

eventual contribution of higher-order waves or the photon-meson current interaction term deriving from an OPE diagram (6). In most of the cases, however, the fit was no better. The only exceptions are the IV, V and VI intervals ($0.6\ \mathrm{GeV} \leqslant E_\gamma \leqslant 0.75\ \mathrm{GeV}$), where a good fit was also obtained at the third order in $\cos\theta$.

Figure 16 shows the coefficients of the expansion (3) *vs.* the photon energy. As one can see, the coefficient A_2 is significantly different from zero only in the central zone of energy, while A_1 has a minimum in the same zone. This behaviour could again indicate the presence of some effect which, however, is not matched by the presently available models or theories.

4·3. *Isobar excitation mechanism.* – We also tried to analyse our data concerning the decay angular distributions of the Δ-isobar at various photon energies by means of the resonant model. This analysis was already carried out with our preliminary data (3). We report here again briefly the arguments and the hypothesis on which the calculation of the expected distributions is based and apply them to the present data with improved statistics, which allows us to split the whole energy range in ten intervals.

If one assumes first that reaction (1) goes entirely through an isobar excitation, which, in order to explain the measured production ratio

$$R = \frac{\pi + \mathrm{p} \to \Delta^0 + \pi^+}{\pi + \mathrm{p} \to \Delta^{++} + \pi^-} \leqslant \frac{1}{9},$$

must have $T = \frac{1}{2}$, and secondly, for the sake of simplicity, that the contribution of Δ^0 is negligible, then the distribution of the photon angle in the Δ-isobar rest system, with respect to the direction of the Δ-isobar itself in the total c.m.s., can be calculated (7).

In order to obtain this angular distribution, a Lorentz transformation should be done, which could change the Δ polarization and, by consequence, the final angular distribution. To overcome this difficulty a rotation can be made so that the axis coincides with the Δ-isobar direction in the total c.m.s. By so doing the Adair approximation is no longer needed.

The calculated distributions were integrated over the photon energy, as well as over all the π^- angles (in the overall c.m.s.) and momenta, and over the other angle φ of proton emission in the Δ-isobar rest system. In Fig. 17 the experimental angular distributions, for the events with $1.150\ \mathrm{GeV/c^2} < M(\mathrm{p}\pi^+) < 1.300\ \mathrm{GeV/c^2}$, are shown for the different energy intervals. The

(6) M. J. MORAVCSIK: *Phys. Rev.*, **104**, 1451 (1956).
(7) I. GIANNINI and A. SANTRONI: *Nuovo Cimento*, **45** A, 359 (1968).

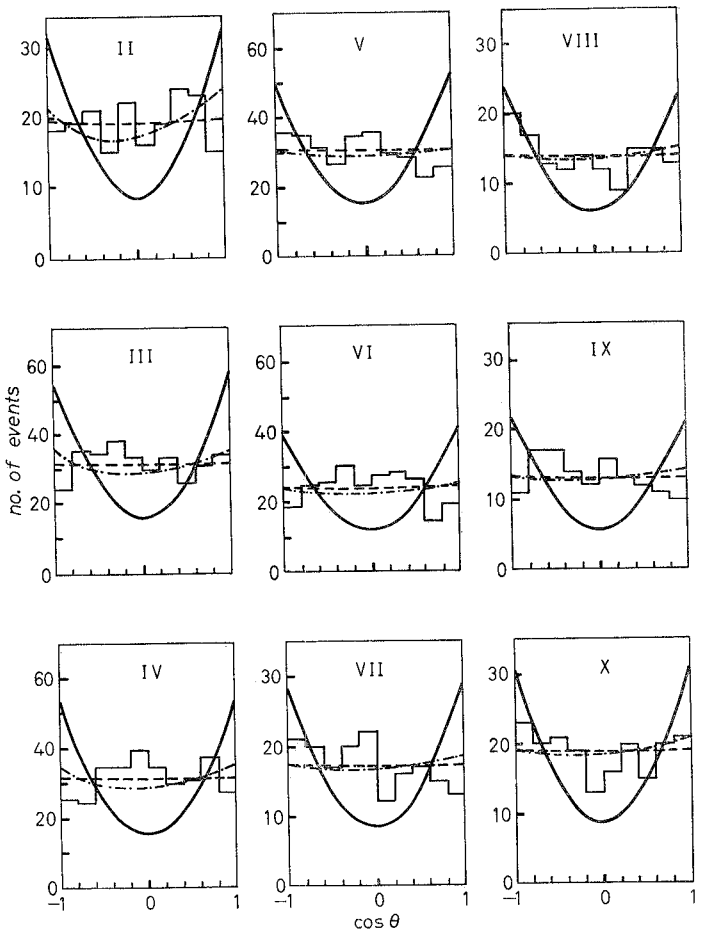

Fig. 17. – Angular distributions of the proton in the Δ^{++}-isobar rest system with respect to the direction of the Δ^{++}-isobar itself in the overall c.m.s. for the various energy intervals of Table I. The curves have been calculated by means the resonant model with different mixtures of D_{13} and P_{11} states: —— P_{11}; — — — D_{13}; —·—·— $1P_{11}+1D_{13}$ (see text).

reported curves represent some calculated distributions, with the condition that the intermediate state be a pure P_{11}-state ($M=1420$ MeV, $\Gamma=100$ MeV), or a pure D_{13}-state ($M=1525$ MeV, $\Gamma=75$ MeV) or a mixture of these taking into account the interference effects.

As one can see, a predominant P_{11}-state excitation in the channel $P_{11}\to\Delta^{++}+\pi^-$ can be excluded, while the discrimination is poor against a small presence of P_{11} with respect to the D_{13}.

A choice was attempted by fitting our experimental data to the various curves. The results are reported in Table II.

TABLE II. – *Results of the best fit of the proton angular distribution obtained with different mixtures of* D_{13} *and* P_{11}. In the first column the relative strength of the D_{13}-state and P_{11}-state is reported. The energy intervals are the same as in Table I. The quoted values are χ^2/n (n = number of degrees of freedom).

$D_{13}:P_{11}$	E_γ interval									
	I	II	III	IV	V	VI	VII	VIII	IX	X
0:1	1.25	2.84	4.5	5.74	5.24	5.55	2.80	1.45	2.67	2.13
1:3	1.02	1.54	1.86	2.44	1.42	1.58	0.91	0.80	1.26	1.0
1:2	0.95	1.13	1.19	1.57	1.23	1.32	0.82	0.77	1.06	0.93
1:1	0.92	0.64	0.75	0.88	1.10	1.15	0.76	0.76	0.89	0.78
2:1	0.93	0.53	0.66	0.71	1.05	1.10	0.73	0.74	0.83	0.87
5:1	0.93	0.53	0.64	0.67	1.03	1.09	0.72	0.73	0.79	0.85
1:0	0.93	0.53	0.63	0.67	1.02	1.08	0.72	0.73	0.78	0.84

5. – The two-pion system.

Since 1962 many experiments have shown the existence of anomalies in the mass distribution of the $(\pi^+\pi^-)$ system between the threshold and the ρ-meson mass. Conversely, there is an almost equal number of experiments which do not show any effect or in which the positions of the bumps seem not to be fixed, but instead to depend on the kinematical conditions. It is evident that the situation is absolutely unclear, in spite of the great deal of both experimental and theoretical work which has been done.

As regards the photoproduction process, in a previous counter experiment at Frascati some evidence of the existence of a resonant state (the so-called σ-meson, $M = 400$ MeV, $T = J = 0$) was found [8].

In Fig. 18 the mass distributions of the $(\pi^+\pi^-)$ system are reported, together with the curves calculated by adding the expected percentage of phase space to the Δ^{++} contribution in this channel. The agreement between the experimental and calculated distribution is noticeable, and we do not observe any enhancement which could imply the existence of a $(\pi^+\pi^-)$ resonance. Moreover, the significant difference between the π^+ and π^- angular distributions (see Fig. 19) rules against an interpretation of the data in terms of the decay of an intermediate state (say P_{11}) into proton plus σ, as suggested by LOVELACE [9], in fact, because of the σ quantum numbers, this would imply equal distributions for the two pions.

---

[8] R. DEL FABBRO, M. DE PRETIS, R. JONES, G. MARINI, A. ODIAN, G. STOPPINI and L. TAU: *Phys. Rev.*, **139** B, 701 (1965).

[9] C. LOVELACE: *Pion-nucleon phase shifts*, invited paper at the 1966 Berkeley Conference.

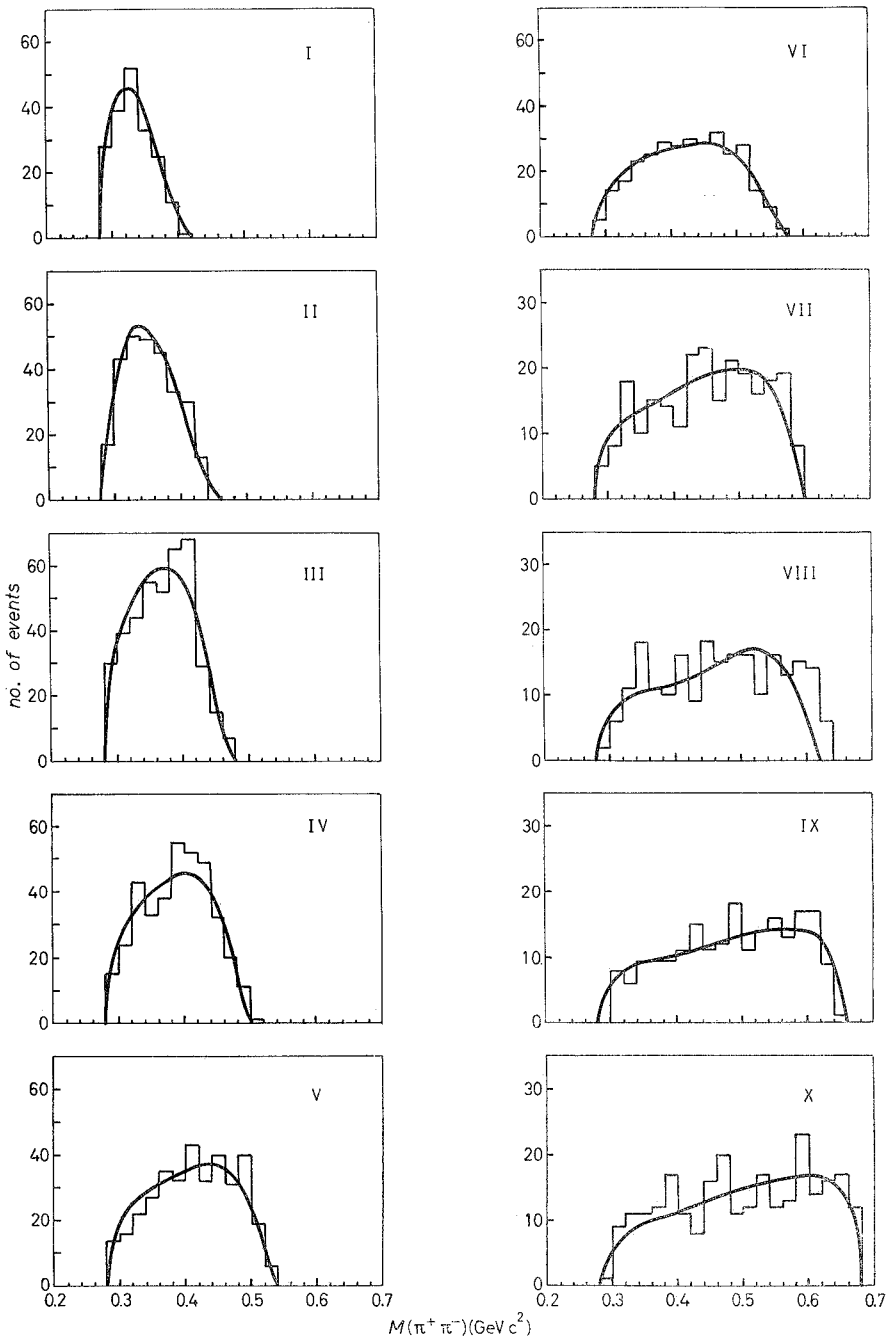

Fig. 18. – Distributions of the $(\pi^+\pi^-)$ equivalent mass for the different photon energy intervals of Table I. The curves represent the calculated distributions taking into account the reflection of the Δ^{++}-isobar.

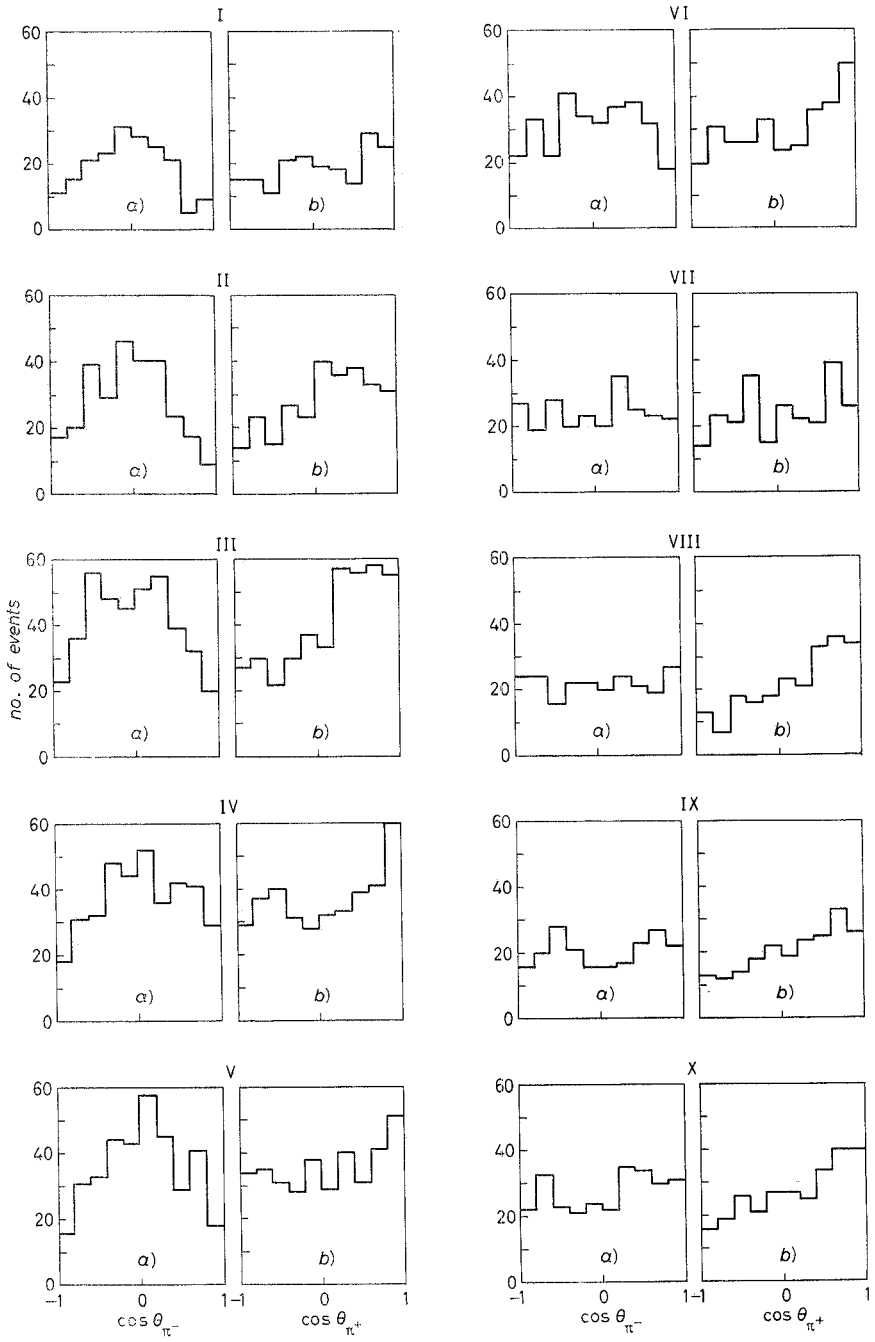

Fig. 13. - Angular distributions in the overall c.m.s. of the pions for the different photon energy intervals of Table I. *a*) cos θ_{π^-}, the cosine of the angle between the π^- and the photon directions; *b*) cos θ_{π^+}, the corresponding angle for the π^+.

6. – Conclusions.

We have reported the final result of an analysis of the photoproduction process of two charged pions on proton. This investigation is now being extended by our group to the other double photoproduction reactions on neutron and proton by means of deuterium and heavy-liquid bubble chambers, so that a complete experimental picture will be available.

As far as the reaction $\gamma+p\to p+\pi^+ +\pi^-$ is concerned, the main features, below 1000 MeV, can be summarized as follows:

a) The total cross-section increases rapidly with the energy. It reaches a maximum at 650 MeV and then remains about constant.

b) There is a very abundant production of the Δ-isobar in the $\Delta^{++}(\pi^+ p)$ charge state, while the production percentage of its neutral charge state $(\pi^- p)$ is very low.

c) The total cross-section of Δ-isobar production shows a peak at 650 MeV, which may be due to a resonant state. In this energy interval also the Δ angular distribution (c.m.s.) is modified. These facts suggest trying to fit the data with the isobar excitation model, the intermediate state having $T=\frac{1}{2}$. However while an analysis of the decay angular distribution of the Δ-isobar certainly excludes a predominant P_{11} channel, our present data do not allow us to draw definite conclusions on the formation of this resonance in the investigated reaction.

d) The mass distributions of the $(\pi^+\pi^-)$ system do not show any enhancement which may be attributed to a $(\pi^+\pi^-)$ resonance with mass below 600 MeV/c^2.

Finally, we want to stress that the actual interpretation of our experimental data is not yet satisfactory, because some unsolved questions require a comparison with the data on all the other double photoproduction processes. We think, therefore, that the situation will become clearer after all the complementary processes have been investigated by us in the bubble chamber experiments which we are presently carrying on.

* * *

We are grateful to the European Organization of Nuclear Research (CERN) for having lent us the bubble chamber and to Prof. L. MEZZETTI, who made possible its installation at the Laboratori Nazionali del CNEN in Frascati. We are obliged to the Synchrotron and Cryogenic Laboratory staffs for their collaboration during the runs. Furthermore we wish to thank our technicians Messrs. P. BENVENUTO, A. DELLA CIANA, D. FABBRI, M. MAGRINI and L.

MAIANI for their indispensable assistance during the chamber assembling and exposure, and the scanning team for the careful analysis of the pictures.

The assistance of Drs. A. DI LAZZARO and A. MAGGIOLO (CNAF, Bologna) and of Mr. E. VALENTE and MR. VIAGGI in the data processing calculations is also gratefully acknowledged.

RIASSUNTO

Si riportano i risultati finali di un esperimento di fotoproduzione di due pioni carichi su protone dalla soglia a 1000 MeV. La caratteristica predominante è la produzione molto abbondante dell'isobaro nello stato di carica $\Delta^{++}(\pi^+p)$ e la bassa percentuale di produzione del suo stato neutro (π^-p). Questo fatto, insieme con il picco mostrato, per $E_\gamma = 650$ MeV, dalla sezione d'urto totale di produzione, suggerisce di analizzare i dati secondo un meccanismo di eccitazione di uno stato intermedio con $T = \frac{1}{2}$ Conclusioni definitive sulla formazione della risonanza P_{11} non possono peraltro essere ottenute. Le distribuzioni angolari di produzione del Δ^{++} sono bene approssimate da un polinomio di secondo grado in $\cos\theta$. La distribuzione della massa equivalente del sistema $(\pi^+\pi^-)$ non mostra nessuna deviazione che possa essere attribuita a una risonanza $(\pi^+\pi^-)$ con massa inferiore a 600 MeV/c^2.

Анализ реакции $\gamma+p \to p+\pi^++\pi^-$ при энергиях вплоть до 1 ГэВ в водородной пузырьковой камере.

Резюме (*). — Сообщаются окончательные результаты эксперимента по фоторождению двукратно заряженных пионов на протонах при энергиях вплоть до 1 ГэВ. Наиболее поразительной особенностью является очень обильное рождение Δ-изобары в $\Delta^{++}(\pi^+p)$ зарядовом состоянии и очень низкий процент рождения этой изобары в нейтральном зарядовом состоянии (π^-p). Этот факт, вместе с очевидным пиком полного поперечного сечения при E_γ=650 МэВ, предлагает попытаться подогнать полученные данные с помощью модели изобарного возбуждения, причем, промежуточное состояние имеет $T=\frac{1}{2}$. Однако, точные заключения об образовании резонанса P_{11} не могут быть получены. Получается хорошая подгонка угловых распределений Δ^{++} рождения с помощью полиномов второго порядка по $\cos\theta$. Распределение масс для системы $(\pi^+\pi^-)$ не обнаруживает никакого увеличения, которое можно было бы приписать резонансу $(\pi^+\pi^-)$ с массой ниже 600 МэВ/c^2.

(*) *Переведено редакцией.*